

# Changes in lake area and water level in response to hydroclimate variations in the source area of the Yellow River: a case study from Lake Ngoring

Yang PU (✉)<sup>1</sup>, Min ZHAN<sup>1</sup>, Xiaohua SHAO<sup>1</sup>, Josef P. WERNE<sup>2</sup>, Philip A. MEYERS<sup>3</sup>,  
Jiaojiao YAO<sup>1</sup>, Da ZHI<sup>1</sup>

<sup>1</sup> School of Geographical Sciences, Nanjing University of Information Science & Technology, Nanjing 210044, China

<sup>2</sup> Department of Geology and Environmental Science, University of Pittsburgh, Pittsburgh PA 15260, USA

<sup>3</sup> Department of Earth and Environmental Sciences, The University of Michigan, Ann Arbor MI 48109, USA

© Higher Education Press 2023

**Abstract** In the north-eastern Qinghai-Tibet Plateau (QTP), the source area of the Yellow River (SAYR) has been experiencing significant changes in climatic and environmental conditions in recent decades. To date, few studies have combined modern hydrological conditions with paleoclimate records to explore the mechanism(s) of these changes. This study seeks to improve understanding of hydrological variability on decadal and centennial timescales in the SAYR and to identify its general cause. We first determined annual fluctuations in the surface area of Lake Ngoring from 1985 to 2020 using multi-temporal Landsat images. The results show that lake surface area changes were generally consistent with variations in precipitation, streamflow and the regional dry-wet index in the SAYR, suggesting that the water balance of the Lake Ngoring area is closely associated with regional hydroclimate changes. These records are also comparable to the stalagmite  $\delta^{18}\text{O}$  monsoon record, as well fluctuations in the Southern Oscillation Index (SOI). Moreover, an association of high TSI (total solar insolation) anomalies and sunspot numbers with the expansion of Lake Ngoring surface area is observed, implying that solar activity is the key driving factor for hydrologic variability in the SAYR on a decadal timescale. Following this line of reasoning, we compared the  $\delta^{13}\text{C}_{\text{org}}$ -based lake level fluctuations of Lake Ngoring for the last millennium, as previously reported, with the hydroclimatic history and the reconstructed TSI record. We conclude that the hydrological regime of Lake Ngoring has been mainly controlled by centennial fluctuations in precipitation for the last millennium, which is also dominated by solar activity. In general, it appears that solar activity has

exerted a dominant influence on the hydrological regime of the SAYR on both decadal and centennial timescales, which is clearly manifested in the variations of lake area and water level of Lake Ngoring.

**Keywords** Qinghai-Tibet Plateau (QTP), source area of the Yellow River (SAYR), lake area/level, Asian summer monsoon (ASM), El Niño-Southern Oscillation (ENSO), total solar insolation (TSI)

## 1 Introduction

The Qinghai-Tibetan Plateau (QTP) is the world's largest high-altitude plateau, and it is known as the "roof of the world" and the "third pole" (Kang et al., 2010). Because the climate of the QTP is heavily influenced by the Asian summer monsoon (ASM) and closely associated with the El Niño-Southern Oscillation (ENSO), it is particularly vulnerable to changes in global climate (Liu et al., 2009; Liu et al., 2020). Changes in lake area/level are important indicators of climate change and may correlate with regional hydrological regimes, thereby reflecting the dynamics of water balance (Mason et al., 1994; Zhang et al., 2019a; Zhang et al., 2020). Meanwhile, many studies have reconstructed past lake level changes using geochemical indicators in lacustrine sediments, such as the  $\delta^{18}\text{O}$  values of fossil ostracods (e.g., Lister et al., 1991), *n*-alkane proxies (e.g., Pu et al., 2009), organic carbon isotopes (e.g., Liu et al., 2013), and microbial lipids (glycerol dialkyl glycerol tetraethers, or GDGTs; e.g., Wang et al., 2019). However, recent studies that have combined these two research directions together are extremely rare.

The Yellow River originates from the north-east part of

the QTP and is the second longest river in China. The source area of the Yellow River (SAYR) refers to the catchment above the Tangnaihe gauging station of the main stem of the Yellow River. The SAYR plays an important role in climate regulation and water conservation on the north-eastern QTP. However, global warming has led to an increase in temperature in the SAYR and has resulted in a series of environmental issues related to climate anomaly variations and ecological degradation (Guo et al., 2022). Having a thorough understanding of hydroclimate changes in the SAYR will contribute meaningfully to regional social development and economic stability. Previous studies have suggested that the climate in the SAYR has experienced a significant increasing warm-wet trend since the early 2000s, which is very different from the antecedent warm-arid trend since the late 1980s (Luo et al., 2020). The result of this increase is permafrost deterioration, rising groundwater levels, expansion of lakes and wetlands, and transition of grassland ecosystems from steppes to alpine meadows in the SAYR. Nevertheless, it remains unclear how climate factors including solar irradiation, temperature, precipitation, and dry-wet conditions influence hydrological regimes in the SAYR and how these factors interact, leading to discrepancies in quantitative forecasts of hydrological variability in the north-eastern QTP (Meng et al., 2016).

Lake Ngoring is the largest lake in the SAYR and serves as a natural reservoir that absorbs the spring flood peak and regulates the annual discharge budget of the Yellow River (Kirillin et al., 2017) (Fig. 1(a)). Earlier studies suggested that the hydrological conditions in QTP lakes are affected by local precipitation patterns, surface runoff, meltwater contributions from adjacent glaciers, and the intensity of evaporation relative to precipitation, and that groundwater-lake exchange has had a very small impact on water balance in this lake (Lei et al., 2013). However, changes in the relationship between climate

evolution and hydrological variability in such large lakes are not fully understood and merit further investigation.

Herein, we describe our investigation of the factors involved with surface area and water level changes of Lake Ngoring and related hydroclimate change in the SAYR, exploring whether similar mechanisms exist across different timescales. We retrieved the history of Lake Ngoring surface area during the past 36 years by using multi-temporal Landsat images and compared it with the precipitation amounts, streamflow, dry-wet conditions, and ASM variability based on stalagmite  $\delta^{18}\text{O}$  from the Wanxiang Cave, the Southern Oscillation Index (SOI), and the total solar insolation (TSI). Also, we compared the  $\delta^{13}\text{C}_{\text{org}}$ -based lake level changes with reconstructed suspended sediment load (SSL), dry-wet conditions, and regional precipitation in the SAYR as well as the total solar insolation (TSI) for past 1500 years, reasoning that the regional precipitation and dry-wet conditions could result in lake level oscillations.

## 2 Study area and methods

### 2.1 Study area

The SAYR covers an area of  $12.2 \times 10^4 \text{ km}^2$  and accounts for 16% of the Yellow River basin. The mean annual streamflow in this area is  $20.52 \times 10^9 \text{ m}^3$ , which accounts for almost 38% of the natural runoff of the Yellow River basin (Hu et al., 2011). Consequently, the SAYR is called “the water tower of the Yellow River” (Zheng et al., 2009).

Lake Ngoring ( $34^\circ46'$  to  $35^\circ05'$  N,  $97^\circ54'$  to  $99^\circ32'$  E) is in Madoi County, at an elevation of 4272 m and is a typical tectonic lake situated between the Buqing Mountains to the north and the Bayan Har Mountains to the south (Pu et al., 2020) (Figs. 1 and 2). The lake is a typical alternately inflow-outflow lake (river-connected lake) and has a surface area of about  $620 \text{ km}^2$  (long-time

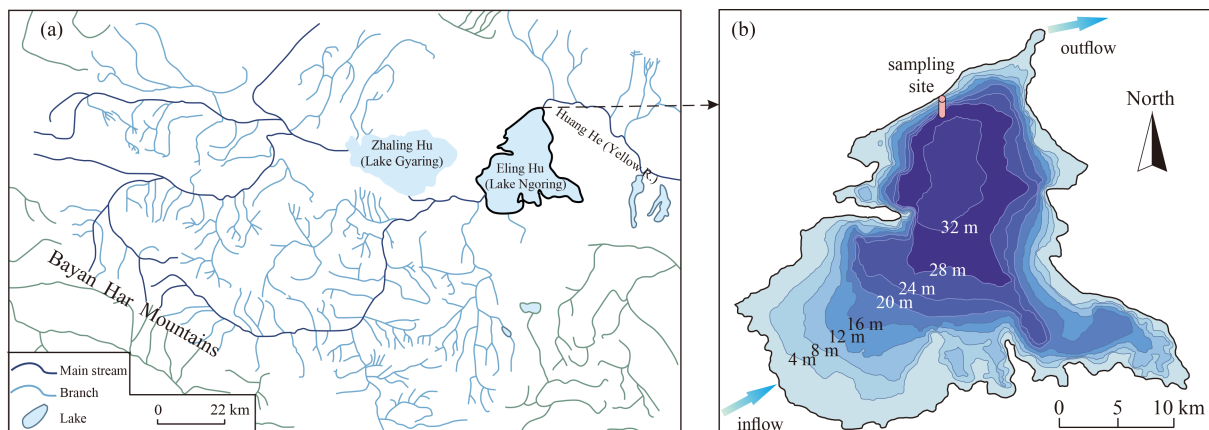


**Fig. 1** The drainage system distribution of the study area (Lake Ngoring is marked by thick solid lines) (a), and a contoured bathymetric map of Lake Ngoring where the site of the sediment core sampled is marked (redrawn from Pu et al., 2020) (b).

average annual value) with a catchment area of 18188 km<sup>2</sup>, making it the largest lake in the SAYR.

A cold and semi-arid continental climate prevails in the lake basin. The mean daily air temperature varies from 7.7°C in July to −16.2°C in January, annually averaging −3.0°C (1985–2020), and the annual precipitation averages 345.6 mm (1985–2020). During the period of late November through early April, the surface of the lake is completely covered in ice, thereby isolating the lake ecosystem from the surrounding environment (Fig. 2(b)).

In the SAYR, due to the harsh environment (e.g., the cold and arid climate, increased radiation exposure, lower atmospheric oxygen availability at high elevation), terrestrial plants suffer a significant impact on their growth and distribution. The main vegetation types in the SAYR are alpine meadow and steppe in the plains area and sparse vegetation in the high elevation area (Jin et al., 2009). The vegetation around Lake Ngoring is composed of high elevation cold-steppe species that are dominated by C<sub>3</sub> grasses such as *Stipa purpurea* and *Poa annua*, which provide good herbage for animal husbandry in the region. Around the lake shore, emergent aquatic plants and subaerial plants are sparse, which helps to distinguish the outline of Lake Ngoring from remote-sensing images (Fig. 2).

## 2.2 Data source and methods

### 2.2.1 Sources of satellite data and methods of lake mapping

NASA and the US Geological Survey jointly manage the Landsat satellite missions that have been widely used to map water bodies since 1972. We obtained moderate resolution images from these missions, including 60 m for MSS (Multispectral Scanner, Landsat 4) and 30 m for TM (Thematic Mapper, Landsat 4-5), ETM+ (Enhanced Thematic Mapper Plus, Landsat-7), and OLI (Operational Land Imager, Landsat-8). The Landsat missions provided the most comprehensive lake area observations over the QTP. With the exceptions of products lacking during the early stage and the lake area being impossible to determine in some years due to image blur, the available products are normally usable since 1985. This study used

Landsat MSS, TM, ETM<sup>+</sup>, and OLI images from 1985 to 2020 as the remote sensing data sources for investigating lake area variations. We selected remote sensing images that had little or no cloud cover, mostly during the months of September to November, when the lake area is relatively stable after the rainy season that lasts from June to August in Madoi County. The Landsat data were acquired from the USGS Earth Explorer website, and all images were spectrally and radiometrically calibrated and atmospherically corrected by ENVI 5.3 before being used for lake area mapping in ArcMap 10.7.

McFeeters (1996) proposed the use of the Normalized Difference Water Index (NDWI) for extracting the water body based on the spectral analysis that water absorbs most of the near and mid-infrared bands and reflects the visible band. It is a band ratio index between the green and near-infrared (NIR) spectral bands, which can improve the spectral characteristics of water bodies and suppress background noise (Xu, 2006). The water extraction threshold of Ngoring Lake is then obtained by artificial visual interpretation to separate water bodies and non-water objects. NDWI is defined as

$$NDWI = \frac{(Band_{green} - Band_{NIR})}{(Band_{green} + Band_{NIR})}, \quad (1)$$

where Band<sub>green</sub> is the reflectance in the green band, and Band<sub>NIR</sub> is the reflectance in the near-infrared band.

### 2.2.2 Acquisition of the meteorological, streamflow, TSI, and sunspot data

The China meteorological data service center provided the observation data of precipitation at the Madoi Meteorological Station (1985–2020), the closest meteorological station to Lake Ngoring. The annual streamflow data (1955–2019) were measured at Huangheyuan gauging station (98°10′ E; 34°53′ N, 4035 m a.s.l.), which was provided by the Yellow River Conservancy Commission, Ministry of Water Resources. This station is the first gauging station along the Yellow River and is the nearest one to Lake Ngoring. The NOAA National Centers for Environmental Information provided the annual TSI and SOI data for 1980–2020. The

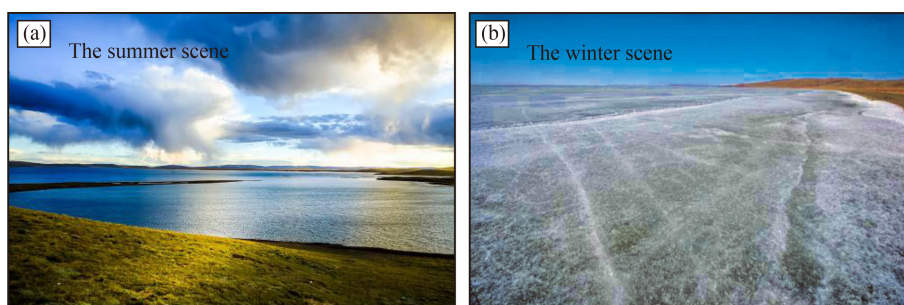


**Fig. 2** The landscape of Lake Ngoring, SAYR, in the summer (a) and winter (b).

international sunspot number data were obtained from the Solar Influences Data Analysis website.

### 2.2.3 Mathematical methods

A conventional detrending method was applied to remove the linear trend from the surface area data of Lake Ngoring by using the detrend function in MATLAB (Zhao et al., 2021). The Mann-Kendall (M-K) mutation test was used to determine the mutational sites of hydroclimatic indices during the past 36 years. The M-K mutation test is commonly used as a nonparametric test of climate parameters (Mann, 1945). It is possible to use this method to determine if there are mutation sites present in a time sequence. A detailed description about the M-K test can be found in Fathian et al. (2016), which also presents time series data of hydrology and climate from a lake basin.

## 3 Results and discussion

### 3.1 Relationship between Lake Ngoring surface area and hydroclimate conditions in the SAYR

Considering that human activity in the SAYR is relatively small, variations in lake area can be used as reliable indicators for natural climate variability (Zhang et al., 2020). Figure 3 shows the changes in the surface area of Lake Ngoring and the detrended area during the period 1985–2020. The smallest lake area for the past 36 years is observed in 1996 (yellow line), and the largest is in 2013 (red line). The lake area has expanded mostly in the south-western part of Lake Ngoring because of the relatively shallow average depth in this zone, whereas the changes in the deep-water zone are less pronounced (Figs. 1(c) and 4). It is easy to speculate that hydroclimate changes result in the lake area fluctuating chiefly in shallow water zones. In contrast, the deep-water zone in a lake is assumed to have less noticeable areal changes even if the hydroclimate conditions varied significantly. Specifically, during the period from 1985 to 2006, the Lake Ngoring surface area remained relatively stable but after 2006 its area increased significantly with obvious oscillations (Fig. 3). This observed pattern is supported by the M-K mutation test, as displayed in Fig. 5(a). A mutation site in lake area changes occurs in 2006, implying that the area of Lake Ngoring increases significantly after that time.

To investigate the relationship between hydroclimatic conditions and lake area on a decadal timescale, we compared lake area changes from 1985 to 2020 (Fig. 6(b)) with the corresponding precipitation record from the Madoi meteorological station (Fig. 6(c)) and the streamflow record from the Huangheyuan gauging station (Fig. 6(a)). Good agreement exists between lake area and

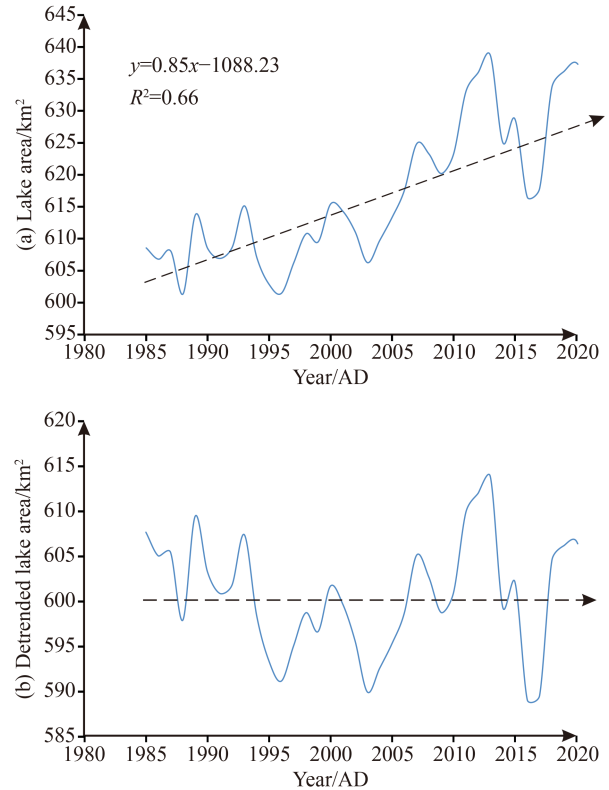


**Fig. 3** Lake surface area changes in Lake Ngoring (a); detrended lake surface area changes in Lake Ngoring (b).

precipitation amount, with a correlation coefficient of 0.47 ( $p < 0.01$ ) (Figs. 6(b) and 6(c); Table 1). Two obvious fluctuations in lake area (highlighted by pink arrows in Fig. 6(b)) correspond well with precipitation changes at the Madoi station (Fig. 6(c)). The three apparent expansions of Lake Ngoring correspond to high phases of precipitation as emphasized by blue shading in Fig. 6. Also, precipitation exhibits four abrupt changes from 2005 to 2008 (Fig. 5(b)), indicating that precipitation significantly increased during this period, which is consistent with the mutation site of lake area changes (Fig. 5(a)). Moreover, the changes in lake area are also closely related to streamflow at the Huangheyuan gauging station, with the  $R$  value reaching 0.52 ( $p < 0.01$ , Table 1, Figs. 6(a) and 6(b)), indicating that large lake area usually corresponds to higher streamflow. The streamflow abruptly increased in 2007 (Fig. 5(c)), immediately after the lake area expanded in 2006 (Fig. 6(a)). With the precipitation increase, the surface runoff in the region experienced an increase. Hence, streamflow in the SAYR is sensitive to changes in precipitation, and these factors exhibit a highly significant correlation coefficient ( $R = 0.65$ ,  $p < 0.01$ ) (Table 1). The agreement between lake area, precipitation amount, and streamflow indicate that precipitation is the main factor affecting the surface area of Lake Ngoring, in accordance with previous studies on the QTP (Lei et al., 2013; Tian

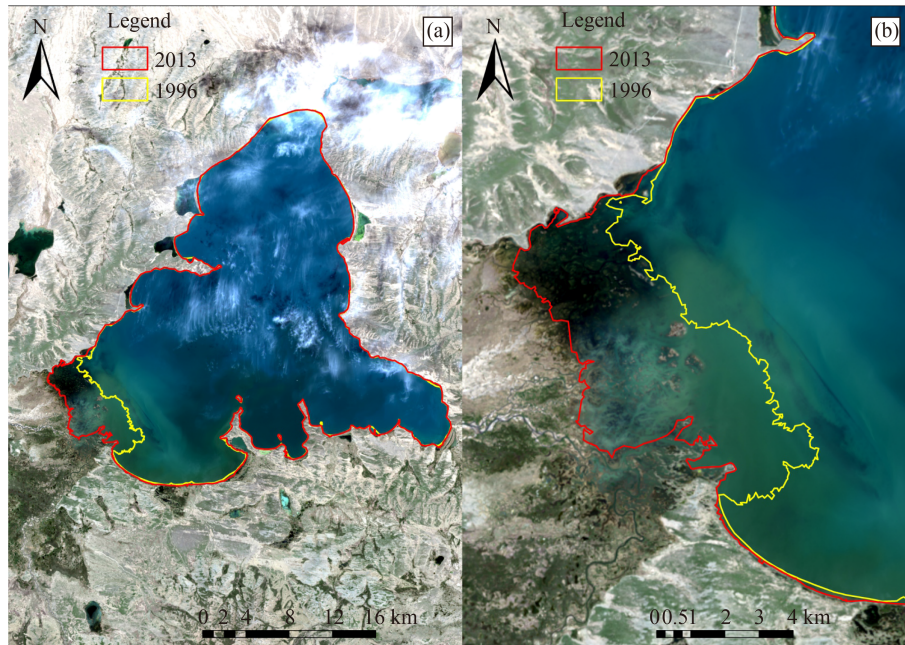


**Fig. 4** Monitoring changes in the surface area of Lake Ngoring using Landsat images from 1985 to 2020. An image comparison between Lake Ngoring in 1996, which has the smallest lake area, and Lake Ngoring in 2013, which has the largest lake area. The left image is the surface area comparison for the whole Lake Ngoring (a); the right image concentrates on the area change in the shallow south-western part of Lake Ngoring (b).

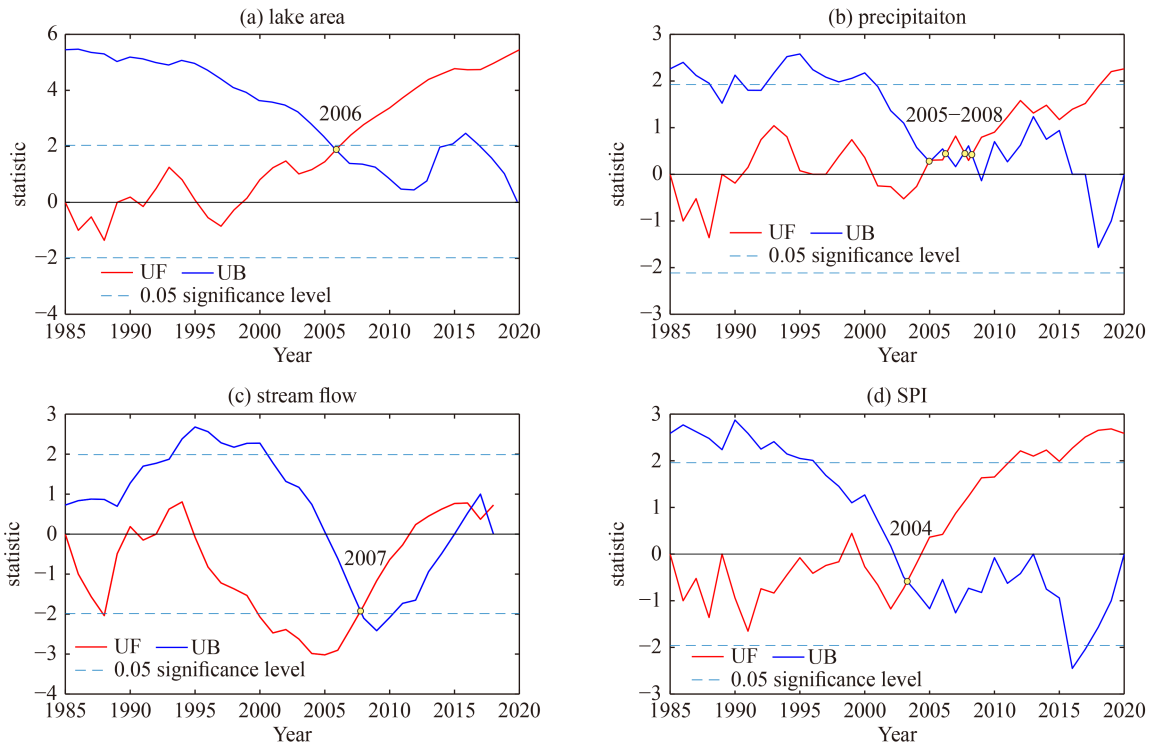


**Fig. 5** A Mann-Kendall (MK) mutation test of the Lake Ngoring area (a); precipitation (b); streamflow (c) and SPI (d) for past 36 years in the SAYR. The yellow points represent the mutation sites where the index sequences display abrupt changes.

et al., 2015; Zhang et al., 2019a, 2019b, 2020).

Considering that Lake Ngoring is the largest lake in the SAYR, its lake area change is likely to be representative and to provide a link with both local precipitation in the

Lake Ngoring catchment and regional dry-wet conditions in the SAYR. The World Meteorological Organization (WMO) officially adopted and recommended a Standardized Precipitation Index (SPI) as a tool for

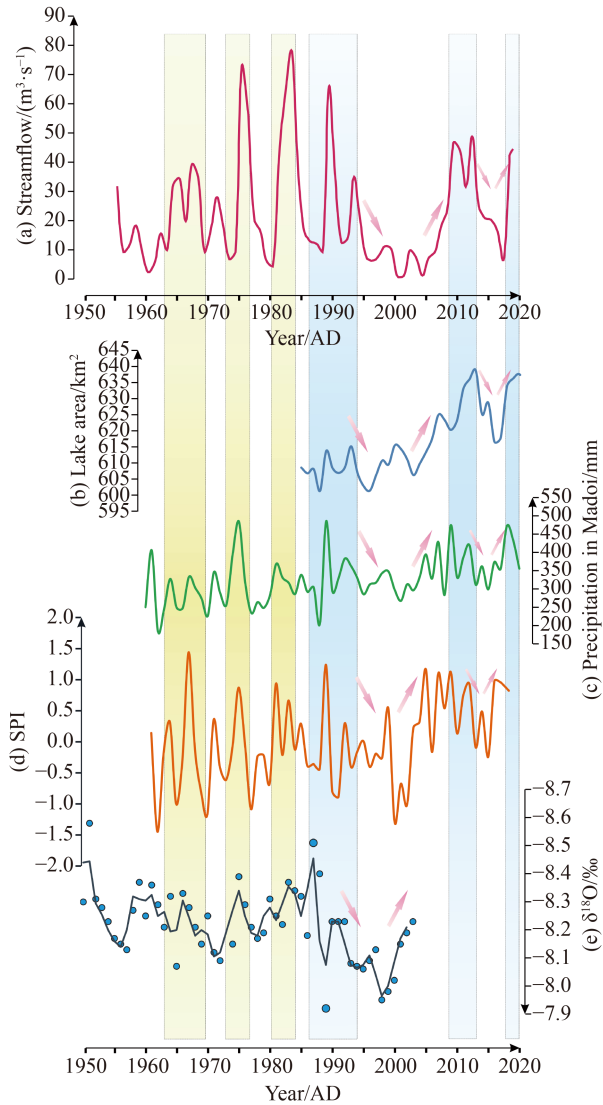


**Fig. 6** Surface area changes in Lake Ngoring (b) compared with streamflow variations at the Huangheyuan gauging station (a), precipitation changes recorded at the Madoi meteorological station (c), SPI variations from 1960 to 2017 in the SAYR (Gu et al., 2019) (d) and the two-point moving average of stalagmite  $\delta^{18}\text{O}$  from Wanxiang Cave at the north-eastern margin of the QTP (Fig. 1(a); Zhang et al., 2008) (e). The blue shading highlights the corresponding phases during the period for which lake area data exists; yellow shading highlights the corresponding phases lacking lake surface area data.

evaluating dry-wet cycles. The SPI was developed to measure drought or humidity over time for a defined area by McKee et al. (1993). The dry-wet conditions in the SAYR from 1961 to 2017 were determined by applying the SPI (Gu et al., 2019) (Fig. 6(d)) based on regional precipitation data from 9 meteorological stations in the area. Changes in SPI appear to be in accord with Lake Ngoring surface area changes ( $R = 0.42, p < 0.01$ , Table 1), and most of the wetter periods are consistent with phases of surface area expansion (Figs. 6(b) and 6(d)). Thus, Lake Ngoring surface area changes agree with the precipitation record and SPI, indicating that lake area of Lake Ngoring is mainly affected by local precipitation and concordant with the regional dry-wet conditions. In addition, the mutation site in SPI changes occurs in about 2004 (Fig. 5(d)), which indicates that the abrupt change in lake surface area and regional dry-wet conditions occurred almost simultaneously, whereas regional wetting trends are expected to precede lake area increases by 1–2 years. In general, comparable trends were observed in lake surface area, precipitation, streamflow, and SPI from 1985 to 2020. Furthermore, the variations in precipitation, SPI, and streamflow displayed comparable trends from 1960 to 2020, although not all the data sets are complete.

It is evident from the preceding discussion that local precipitation along with regional dry-wet conditions are likely the dominant factors affecting the surface area of Lake Ngoring. Paleoclimate studies have also obtained similar results over a long period of time. For instance, the volume of water in Qinghai Lake, which is closely related to the amount of precipitation, has varied with the intensity of the ASM during the late Pleistocene and Holocene (Lister et al., 1991). The records of  $\delta^{18}\text{O}$  values in authigenic carbonates and ostracod shells in the same lake are also consistent with fluctuations in lake level during the past 300 years, which are driven by changes in ASM intensity (Henderson et al., 2003). According to the sedimentary record from Ahung Co in the central QTP, early and middle Holocene lake level fluctuations can be attributed to monsoon precipitation variations (Morrill et al., 2006). In light of these linkages, we used the stalagmite  $\delta^{18}\text{O}$  record from Wanxiang Cave in the north-

**Table 1** Correlation coefficients ( $R$  values) of lake surface area and precipitation data from the Madoi meteorological station, streamflow data from Huangheyuan gauging station, SPI of the SAYR, SOI, and TSI variations. The underlined values are those significant at a 99% level ( $p < 0.01$ )

Item	Lake area	Precipitation	Streamflow	SPI	SOI	TSI
Lake area	1.00					
Precipitation	<u>0.47</u>	1.00				
Streamflow	<u>0.52</u>	<u>0.65</u>	1.00			
SPI	<u>0.42</u>	<u>0.72</u>	<u>0.44</u>	1.00		
SOI	0.24	0.01	0.22	0.12	1.00	
TSI	-0.09	-0.18	0.03	-0.39	0.24	1.00

eastern margin of the QTP (Fig. 1(a)) (Zhang et al., 2008) to represent the intensity of monsoon rainfall in the SAYR. Although the time span of the stalagmite  $\delta^{18}\text{O}$  record does not exceed that of 2003 and is obviously shorter than the other proxies (Fig. 6(e)), the streamflow, precipitation, and SPI changes show good agreement with the stalagmite  $\delta^{18}\text{O}$  variations prior to the availability of satellite derived lake area data (yellow stripes in Fig. 6). It is worth noting that stalagmite  $\delta^{18}\text{O}$  display a pattern of fluctuations very similar to those of lake area, streamflow, precipitation, and SPI sequences (blue stripes in Fig. 6), implying that the surface area of Lake Ngoring is chiefly controlled by precipitation, which is closely associated with the regional monsoon intensity. Thus, phases of lake shrinkage are likely associated with weakening monsoon intensity while phases of lake area enlargement are likely associated with intensified monsoon conditions.

Because Lake Ngoring and all other lakes in the SAYR are totally ice-covered during most of the winter half-year, their surface areas would remain constant during winter. In addition, the SAYR in winter is characterized by severe drought conditions and precipitation is low compared to spring and summer (Li et al., 2016). Thus, the climate factors that dominate in winter such as the westerly jet, the Siberian High atmospheric pressure, and the winter monsoon are not considered, whereas it is believed that the ASM and ENSO are key points for the lake area changes during past 36 years. Previous studies have demonstrated that ENSO-related precipitation plays a significant role in modulating climatic conditions over the QTP region. For instance, it has been highlighted by Wan et al. (2013) that ENSO activity plays a crucial role in determining the nature and seasonality of extreme monthly precipitation levels and suggests that an El Niño year would have lower ASM precipitation than usual on the QTP. Meanwhile, there has been a significant reduction in the size of many lakes on the QTP because of El Niño events in recent decades; the opposite is observed during La Niña years in which the lakes on the QTP grow larger (Lei et al., 2019).

To explore the potential relationship of Lake Ngoring's surface area fluctuations and ENSO activity for past 36 years, we compare the detrended lake area and precipitation record in Madoi County with the Southern Oscillation index (SOI). By using the method of detrending, the linear increased trend is removed from lake area changes during the past 36 years, and focus is placed on observing fluctuations rather than looking at overall trends (Fig. 3(b)). The SOI is the most common index to quantify the difference between sea level pressure of the antiphase oscillatory behavior at Tahiti in the eastern Pacific Ocean and at Darwin in the western Pacific Ocean (Ropelewski and Halpert, 1986). During most of the period, the changes in Lake Ngoring surface area and precipitation variations in Madoi are comparable

with SOI fluctuations, although several years are not concordant (Figs. 7(b), 7(c), and 7(d)). Both the Pearson correlation coefficient between the annual data of lake area and SOI, as well as precipitation and SOI, are extremely low (Table 1). However, we consider that they show similar fluctuations on a decadal timescale (Fig. 7). Higher precipitation and larger surface area in Lake Ngoring generally coincide with positive ENSO activity, which corresponds with the La Niña-like state (blue stripes in the Fig. 7), whereas more drought periods and declining surface area of Lake Ngoring generally correspond to weaker ENSO activity, which corresponds with the El Niño-like state in the SAYR. Therefore, we believe that ENSO activity significantly influences the monsoon precipitation on the QTP, which in turn largely determines changes in lake area in the SAYR.

Pursuing this line of reasoning, the question can be asked if these correspondences could be also observed on a centennial timescale in Lake Ngoring. The following discussion aims to address this issue.

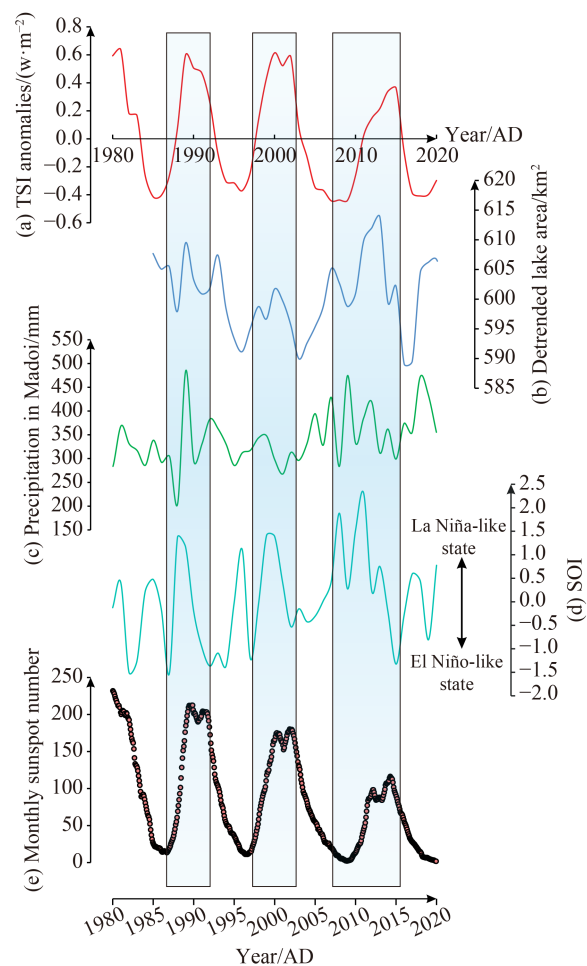


**Fig. 7** Detrended lake surface area of Lake Ngoring (b) compared with TSI anomalies (a), precipitation changes at the Madoi meteorological station (c), annual SOI record (d), and variations in the monthly sunspot number (e).

### 3.2 Significance of changes in bulk organic $\delta^{13}\text{C}$ values in Lake Ngoring sediments over the past 1500 years

A case study of paleolake sediments from the Qaidam Basin, north-eastern QTP, illustrated how sedimentary  $\delta^{13}\text{C}_{\text{org}}$  can track lake level fluctuations in a QTP lake (Pu et al., 2010). We measured the bulk organic  $\delta^{13}\text{C}$  in Lake Ngoring sediments deposited continuously over past 1500 years (Fig. 8(a)) and postulated that the  $\delta^{13}\text{C}_{\text{org}}$  variations associated with the lake level fluctuations are influenced by monsoon activities and ENSO phase evolution (Pu et al., 2020). The conclusions drawn from our previous studies are consistent with very recent advances in lake sediment study. For instance, the variations in sedimentary  $\delta^{13}\text{C}_{\text{org}}$  from 55 freshwater and brackish lakes in mid-latitude Asia show an arched pattern against

lake water depth, although the salinity effect and/or terrestrial  $\text{C}_4$  input in saline lakes with salinity  $> \sim 100000$  mg/L might obscure the relationship between  $\delta^{13}\text{C}_{\text{org}}$  and water depth (Jiang et al., 2021). Climatic and environmental history over the past 1800 years from two alkaline lakes in southern Inner Mongolia, Chagan Nuur and Sangin Dalai Nuur, is reconstructed by a series of physical and geochemical proxies. Positive shifts in  $\delta^{13}\text{C}_{\text{org}}$  values correspond to relatively high lake levels under humid conditions and vice versa (Tian et al., 2022). In the case of Lake Gyaring, another large lake in the SAYR, the average carbon isotope values of black carbon ( $\delta^{13}\text{C}_{\text{BC}}$ ), which is derived from the incomplete burning of biomass or fossil fuels, decreased throughout the Holocene, indicating that lake area expanded during the early and mid-Holocene, followed by shrinkage of the lake in the late Holocene (Ning et al., 2022).

In the present study, we expanded our comparison of  $\delta^{13}\text{C}_{\text{org}}$ -based lake level in Lake Ngoring with published studies, including the reconstructed annual suspended sediment load (SSL) of the SAYR (Xu, 2018), the dry-wet history in the middle and upper reaches of the Yellow River (Zheng and Wen, 2020), and the tree ring record of Dulan, north-eastern QTP (Sheppard et al., 2004) (Fig. 8). We first compare the  $\delta^{13}\text{C}_{\text{org}}$  record in Lake Ngoring with the reconstructed SSL of the SAYR over the past 1500 years (Xu, 2018). These indices are in good agreement (Figs. 8(a) and 8(b)). Previous studies have demonstrated that SSL in rivers typically constitutes most of the sediment load that is associated with precipitation and streamflow in the catchment (e.g., Walling and Fang, 2003; Khosravi et al., 2022). The more abundant precipitation and streamflow in the SAYR is commonly related to elevated lake levels that are considered to correspond to more SSL in the catchment and vice versa (Xu, 2018). Consequently, the relatively higher SSL phases displayed in Fig. 8(b) (marked in the blue shading) generally correspond to less negative values of  $\delta^{13}\text{C}_{\text{org}}$  that indicate higher lake levels, whereas the lower SSL phases are associated with negative shifts in  $\delta^{13}\text{C}_{\text{org}}$ , indicating lower water levels in Lake Ngoring.

By using Chinese historical documents that contain records of drought and flood events, the history of dry-wet fluctuations in the middle and upper reaches of the Yellow River over the past 2000 years was retrieved by Zheng and Wen (2020). It is worth noting that  $\delta^{13}\text{C}_{\text{org}}$ -based lake level variations are also generally in accordance with the dry-wet history of the Yellow River in its middle and upper reaches. This agreement signifies that lake level changes in Lake Ngoring might respond not only to local hydroclimate, but also to regional climatic conditions. Although these two proxies do not exactly agree with each other, the positive excursions of  $\delta^{13}\text{C}_{\text{org}}$  values that indicate high lake levels generally are consistent with humid periods (Figs. 8(a) and 8(c), marked by blue shadows). Therefore, the Lake Ngoring

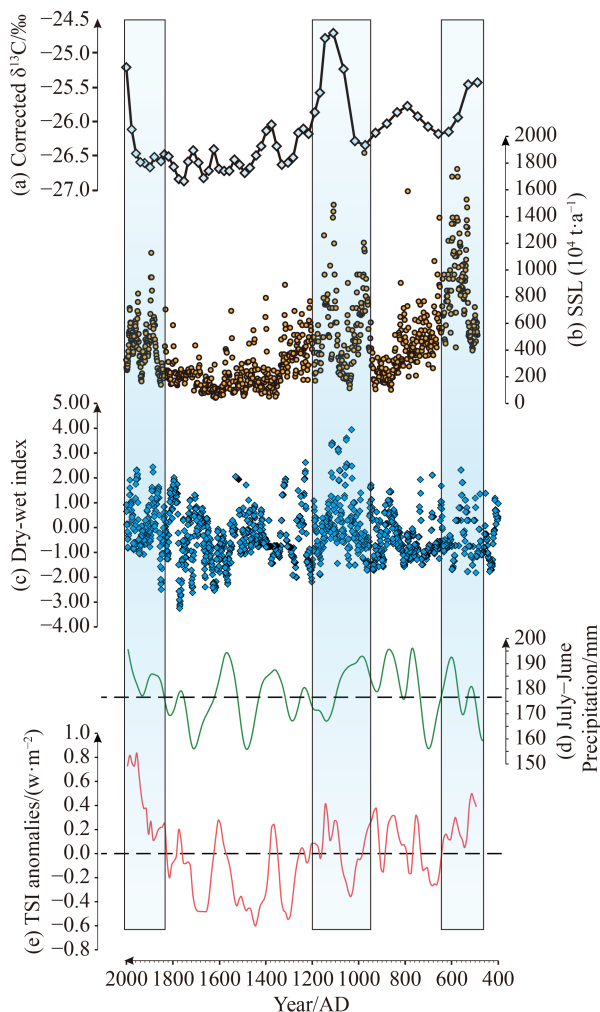


**Fig. 8** The  $\delta^{13}\text{C}_{\text{org}}$  from core NR-1 in Lake Ngoring (Pu et al., 2020) (a) compared with the reconstructed suspended sediment load (SSL) in the SAYR (Xu, 2018) (b), the history of dry-wet fluctuations in the middle and upper reaches of the Yellow River over the past 2000 years (Zheng and Wen, 2020) (c), the July–June precipitation reconstructed from tree rings, Dulan (Fig. 1(a); Sheppard et al., 2004) (d), and the reconstructed TSI for past 1500 years (Vieira et al., 2011) (e).

hydrological regime is closely related to the dry-wet conditions in the middle and upper Yellow River reaches, which is a more extensive geographical range than the SAYR.

Is there any correlation between the  $\delta^{13}\text{C}_{\text{org}}$ -based lake level in Lake Ngoring and regional precipitation patterns? To explore this, we tentatively compared changes in the water level of Lake Ngoring with regional precipitation variations recorded by tree rings in the north-eastern QTP. The July–June precipitation in the Dulan region of the SAYR covering the past 1500 years has been reconstructed from the ring-width index of juniper tree rings (Sheppard et al., 2004) (Fig. 8(d)). The annual resolution of the tree ring record is much greater than that of the sedimentary  $\delta^{13}\text{C}_{\text{org}}$  record shown in Pu et al. (2020), and the tree ring record shows a wider range of temporal oscillations than the  $\delta^{13}\text{C}_{\text{org}}$  record in Lake Ngoring. Consequently, we applied a smoothed line (100-year cubic smoothing spline; Sheppard et al. (2004)) to represent precipitation variations in the SAYR during the past 1500 years. These two records are not consistent in certain periods because QTP lake level variations can be attributed to many factors, and a similar situation is also observed for precipitation. Nevertheless, periods of relatively abundant rainfall roughly correspond to periods of relatively high lake levels (Figs. 8(a) and 8(d), marked by blue shading), indicating the increase in monsoon-related precipitation caused the lake to rise during past 1500 years.

### 3.3 Mechanism of surface area and water level changes in Lake Ngoring and their implications for the SAYR's hydrological environment

As discussed above, the surface area changes for the past 36 years and the reconstructed water level variations in Lake Ngoring are dominated by monsoon intensity and associated with ENSO cycles, but what is the true driving mechanism behind these two? Earlier studies have shown that TSI is probably responsible for the changes in summer monsoon precipitation on multi-year timescales on the QTP (e.g., Tan et al., 2008; Wu et al., 2009; Pu et al., 2010; He et al., 2013; Xu, 2018; Ming et al., 2020). In this study, we observed that positive anomalies in TSI generally correspond to periods with larger lake area and vice versa for the past 36 years (Figs. 7(a) and 7(b)). Meanwhile, a correlation between monthly sunspot numbers and TSI anomalies reveals that decadal-scale cycles dominate solar activity (Figs. 7(a) and 7(e)). The solar insolation and sunspot changes exhibit similar variations with the detrended lake area, indicating that solar activity has periodic cycles that have the same pace as the observed lake area changes. The coincidence between solar cycles and lake area changes during the past 36 years implies that the areal fluctuations of Lake Ngoring are potentially associated with solar activity on a

decadal-scale. However, the correspondences between solar activity and surface area changes in Lake Ngoring may not be so perfect. For example, lake surface area is relatively large from 2006 to 2008 as seen in Fig. 7(b), but the TSI is low. We suggest that lake surface area might be impacted by additional factors, including precipitation, evaporation, streamflow, melting of ice and snow, human activities and their complex response mechanism(s), so the lake surface area changes are unlikely to keep exact pace with solar cycles.

Additionally, TSI changes during the past 1500 years reconstructed by Vieira et al. (2011) are comparable with lake level fluctuations in Lake Ngoring that have been reported in Pu et al. (2020). The  $\delta^{13}\text{C}_{\text{org}}$ -based lake level changes are largely consistent with the TSI anomalies (Figs. 8(a) and 8(e)), which is expected to be dominated by ASM activities and ENSO events in the SAYR that impact regional precipitation and eventually impact lake level (Pu et al., 2020). In general, it is suggested that the water area (level) changes in Lake Ngoring are all influenced by regional hydroclimate factors, including precipitation, regional dry-wet conditions, streamflow in the catchment, and ENSO cycles, and that these factors are ultimately driven by solar activity, both on a decadal-scale and a centennial-scale.

According to other studies, our inference that solar activity is ultimately responsible for the changes in lake area and water level in the SAYR over decadal to centennial timescales is reasonable. For instance, significant fluctuations in lake-level in the Jura and French subalpine ranges and the atmospheric  $^{14}\text{C}$  record during the last 7 millennia show correlation between lake-level rise and high  $^{14}\text{C}$  production and vice versa (Magny, 1993). An association of high sunspot numbers (intense solar activity) with rising lake level in Lake Victoria, East Africa is indicative that solar activity can influence regional rainfall (Stager et al., 2007). The median grain size and  $\delta^{13}\text{C}_{\text{org}}$  record from the Ruogen Co, which is a freshwater alpine lake located in the eastern QTP, indicate lake surface area fluctuations show comparable trends with TSI variations for the last 6 ka (Ming et al., 2020). Although the correspondence between solar activity and lake surface area and water level changes that are reconstructed from proxy-based records have been reported in many paleo-archive studies, we provide the first solid evidence from the exact surface area by using multi-temporal remote sensing images.

To illustrate the mechanism of lake surface area changes in the SAYR, we have drawn a schematic diagram to aid in understanding our results (Fig. 9). With a higher TSI, the ASM would be stronger and bring more precipitation to the north-eastern QTP, causing the lake to expand in the SAYR in accordance with a La Niña-like state. In contrast, an El Niño-like state would occur in the SAYR with a lower TSI, as the ASM would be weaker and bring less precipitation to the north-eastern QTP,

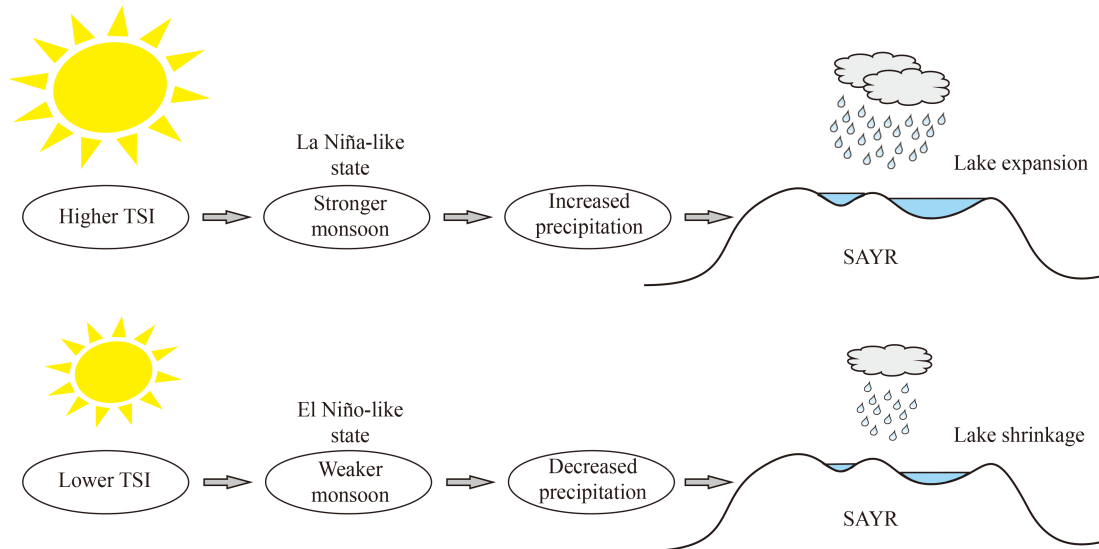


**Fig. 9** Schematic diagram of the mechanism of changing lake surface area in the SAYR.

leading to decreasing lake surface area in the SAYR. Although solar activity fluctuations are relatively weak, their effects on precipitation could be amplified through interactions with sea surface temperatures and atmospheric circulation (Stager et al., 2007). It is likely that the coincidence between solar activity and lake area variation is not random and may indicate a closer dependence between insolation and monsoon activities and associated precipitation in the SAYR. The potential mechanism would be the additive amplification of small thermal effects. Solar warming of land or water surfaces could enhance local convection and precipitation over the SAYR. Also, solar maxima contribute to the warming of the troposphere over most of the planet; this can raise the water vapor content of East Asian onshore winds because of increased marine evaporation and moisture retention (An et al., 2012). As a result, higher humidity could lead to increased precipitation in the SAYR while simultaneously reducing regional evaporation, thereby expanding the lake surface areas. In general, solar activity could play a major role in driving the hydroclimatic fluctuations in the SAYR on different timescales.

Considering all the evidence presented in this study, hydroclimate conditions including precipitation and regional dry-wet conditions are the most important driver of surface area (lake level) of Lake Ngoring, whereas influences derived from human activities in the Lake Ngoring catchment would be minor. However, previous studies emphasized the impact of human activities on the hydrological environment in the SAYR. For instance, by using an optimal desertification monitoring index constructed by Landsat images, desertification in the eastern and southern SAYR showed an increasing tendency during 1995–2015. Anthropogenic activities gradually became the primary factors that aggravated or ameliorated desertification in the SAYR after 2005 (Guo

et al., 2022). Our results support the notion that that hydroclimate factors are the primary drivers of surface area (lake level) fluctuations in Lake Ngoring on decadal to centennial timescale. It is believed that the local economic development and the use of water for human activities do not significantly alter the hydrological regimes of Lake Ngoring. The SAYR seems to have a generally well-protected hydrologic environment, unlike other parts of the Yellow River basin that have a large population.

It must be pointed out that evaporation of lake water and melting of glaciers and snow are not discussed in this study, although they are important for lake water balance on the QTP (Song et al., 2014). Lake Ngoring is a typical open lake and has a low evaporation rate due to the low environmental temperature, which annually averages  $-3^{\circ}\text{C}$ , and ice-covered surface from late November to next early April, preventing any evaporation during this period. Also, a previous study has demonstrated that the slight increase in evaporation in the SAYR caused by global warming was not statistically significant (Liu and Zeng, 2004). Comparing with regional precipitation also suggests that lake evaporation is not a dominant factor for the spatial difference of lake dynamics in the QTP interior (Lei et al., 2014). As for meltwater from glaciers and snow in the study area, the Utah Energy Balance snowmelt model constructed by Tian et al. (2021) highlights that the amount of snowmelt constitutes only 4% of the total surface runoff in the SAYR and only a small amount of runoff may flow into the lakes. From the further estimation of lake water balance on the QTP, it is suggested that increased precipitation is the primary cause (74%) of lake surface area increase, followed by loss of glacier mass (13%) (Zhang et al., 2017). Thus, glacial and snow meltwater are considered to have minimally affected lake area in the SAYR. Despite emphasizing the

key role of precipitation and regional dry-wet conditions in this study, we do not discount the potential importance of evaporation and glacial/snow meltwater in the Lake Ngoring water balance. Future research into lake hydrology in the SAYR requires a more detailed assessment that considers all hydrological factors.

## 4 Conclusions

Changes in lake surface area and water level in Lake Ngoring provide a link to understanding the relationship between climate change and hydrological regime change. Investigations of Lake Ngoring, which is the largest lake in the SAYR, reveal that its hydrological regime is influenced by hydroclimate factors over decadal and centennial timescales. Maximum lake surface area and level were reached during the most intense phase of the ASM under La Niña-like states while lake lowstands have been associated with the diminished precipitation during the weakened ASM phases under El Niño-like states. We postulate that the primary cause for changes in lake surface area and level of Lake Ngoring is the monsoon precipitation in the SAYR that is ultimately related to solar activity. In general, the following sequence might exist: intensified (or weakened) solar activity → strengthened (weakened) ASM → increased (decreased) precipitation → increased (decreased) streamflow → increased (decreased) lake area and rising (falling) water levels in the SAYR. By bringing a new perspective to the study of modern processes and to paleoclimate records, our investigation has tried to bridge existing gaps between these two different avenues of research.

**Acknowledgments** This work was supported by the National Natural Science Foundation of China (Grant Nos. 42171160 and 42172205). We thank three anonymous reviewers for their thoughtful and constructive comments that greatly helped us to improve this manuscript.

**Competing interests** The authors declare that they have no competing interests.

## References

- An Z, Colman S M, Zhou W, Li X, Brown E T, Jull A J T, Cai Y, Huang Y, Lu X, Chang H, Song Y, Sun Y, Xu H, Liu W, Jin Z, Liu X, Cheng P, Liu Y, Ai L, Li X, Liu X, Yan L, Shi Z, Wang X, Wu F, Qiang X, Dong J, Lu F, Xu X (2012). Interplay between the Westerlies and Asian monsoon recorded in Lake Qinghai sediments since 32 ka. *Sci Rep*, 2(1): 619
- Fathian F, Dehghan Z, Bazrkar M H, Eslamian S (2016). Trends in hydrological and climatic variables affected by four variations of the Mann-Kendall approach in Urmia Lake basin, Iran. *Hydrol Sci J*, 61: 892–904
- Gu X, Si J, Lu S, Gui Z, Xie D, Zhao Z, Li S, Li H, You Q (2019). Analysis of dry and wet change characteristics of source region of the Yellow River in historical period. *Jiangsu Agric Sci*, 47(23): 307–312 (in Chinese)
- Guo B, Wei C, Yu Y, Liu Y, Li J, Meng C, Cai Y (2022). The dominant influencing factors of desertification changes in the source region of Yellow River: climate change or human activity? *Sci Total Environ*, 813: 152512
- Henderson A C G, Holmes J A, Zhang J, Leng M J, Carvalho L R (2003). A carbon- and oxygen- isotope record of recent environmental change from Qinghai Lake, NE Tibetan Plateau. *Chin Sci Bull*, 48(14): 1463–1468
- He Y, Liu W, Zhao C, Wang Z, Wang H, Liu Y, Qin X, Hu Q, An Z, Liu Z (2013). Solar influenced late Holocene temperature changes on the northern Tibetan Plateau. *Chin Sci Bull*, 58(9): 1053–1059
- Hu Y, Maskey S, Uhlenbrook S, Zhao H (2011). Streamflow trends and climate linkages in the source region of the Yellow River, China. *Hydrol Processes*, 25(22): 3399–3411
- Jiang J, Meng B, Liu H, Wang H, Kolpakova M, Krivonogov S, Song M, Zhou A, Liu W, Liu Z (2021). Water depth control on n-alkane distribution and organic carbon isotope in mid-latitude Asian lakes. *Chem Geol*, 565: 120070
- Jin H, He R, Cheng G, Wu Q, Wang S, Lü L, Chang X (2009). Changes in frozen ground in the source area of the Yellow River on the Qinghai-Tibet Plateau, China, and their eco-environmental impacts. *Environ Res Lett*, 4(4): 045206
- Kang S, Xu Y, You Q, Flügel W A, Pepin N, Yao T (2010). Review of climate and cryospheric change in the Tibetan Plateau. *Environ Res Lett*, 5(1): 015101
- Khosravi K, Golkarian A, Melesse A M, Deo R C (2022). Suspended sediment load modeling using advanced hybrid rotation forest based elastic network approach. *J Hydrol (Amst)*, 610: 127963
- Kirillin G, Wen L, Shatwell T (2017). Seasonal thermal regime and climatic trends in lakes of the Tibetan highlands. *Hydrol Earth Syst Sci*, 21(4): 1895–1909
- Lei Y, Yang K, Wang B, Sheng Y, Bird B W, Zhang G, Tian L (2014). Response of inland lake dynamics over the Tibetan Plateau to climate change. *Clim Change*, 125(2): 281–290
- Lei Y, Yao T, Bird B W, Yang K, Zhai J, Sheng Y (2013). Coherent lake growth on the central Tibetan Plateau since the 1970s: characterization and attribution. *J Hydrol (Amst)*, 483: 61–67
- Lei Y, Zhu Y, Wang B, Yao T, Yang K, Zhang X, Zhai J, Ma N (2019). Extreme lake level changes on the Tibetan Plateau associated with the 2015/2016 El Niño. *Geophys Res Lett*, 46(11): 5889–5898
- Li Q, Yang M, Wan G, Wang X (2016). Spatial and temporal precipitation variability in the source region of the Yellow River. *Environ Earth Sci*, 75(7): 594
- Lister G S, Kelts K, Zao C K, Yu J Q, Niessen F (1991). Lake Qinghai, China: closed basin lake levels and the oxygen isotope record for ostracoda since the latest Pleistocene. *Palaeogeogr Palaeoclimatol Palaeoecol*, 84(1–4): 141–162
- Liu C, Zeng Y (2004). Changes of pan evaporation in the recent 40 years in the Yellow River Basin. *Water Int*, 29(4): 510–516
- Liu J, Wang S, Yu S, Yang D, Zhang L (2009). Climate warming and growth of high-elevation inland lakes on the Tibetan Plateau. *Global Planet Change*, 67(3–4): 209–217

- Liu S, Duan A, Wu G (2020). Asymmetrical response of the east Asian summer monsoon to the quadrennial oscillation of global sea surface temperature associated with the Tibetan Plateau thermal feedback. *J Geophys Res: Atmos*, 125(20): e2019JD032129
- Liu W, Li X, An Z, Xu L, Zhang Q (2013). Total organic carbon isotopes: a novel proxy of lake level from Lake Qinghai in the Qinghai-Tibet Plateau, China. *Chem Geol*, 347: 153–160
- Luo D, Jin H, Bense V F, Jin X, Li X (2020). Hydrothermal processes of near-surface warm permafrost in response to strong precipitation events in the headwater area of the Yellow River, Tibetan Plateau. *Geoderma*, 376(D5): 114531
- Magny M (1993). Solar influences on Holocene climatic changes illustrated by correlations between past lake-level fluctuations and the atmospheric  $14\text{C}$  record. *Quat Res*, 40(1): 1–9
- Mann H B (1945). Non-parametric tests against trend. *Econometrica*, 13(3): 245–259
- Mason I, Guzkowska M, Rapley C, Street-Perrott F (1994). The response of lake levels and areas to climatic change. *Clim Change*, 27(2): 161–197
- McFeeters S K (1996). The use of the normalized difference water index (NDWI) in the delineation of open water features. *Int J Remote Sens*, 17(7): 1425–1432
- McKee T B, Doesken N J, Kleist J R (1993). The relationship of drought frequency and duration to time scales. In: *Proceedings of the 8th Conference on Applied Climatology*, Boston, MA, USA, 179–183
- Meng F, Su F, Yang D, Tong K, Hao Z (2016). Impacts of recent climate change on the hydrology in the source region of the Yellow River basin. *J Hydrol Reg Stud*, 6: 66–81
- Ming G, Zhou W, Cheng P, Wang H, Xian F, Fu Y, Wu S, Du H (2020). Lacustrine record from the eastern Tibetan Plateau associated with Asian summer monsoon changes over the past ~ 6 ka and its links with solar and ENSO activity. *Clim Dyn*, 55(5–6): 1075–1086
- Morrill C, Overpeck J T, Cole J E, Liu K, Shen C, Tang L (2006). Holocene variations in the Asian monsoon inferred from the geochemistry of lake sediments in central Tibet. *Quat Res*, 65(2): 232–243
- Ning D, Jiang Q, Ji M, Zheng J, Kuai X, Ge Y, Xu Y, Cheng L, Zhao W (2022). Sedimentary black carbon isotope record of Holocene climate changes on the northeastern Tibetan Plateau. *Paleoceanogr Paleoclimatol*, 37(8): e2022PA004487
- Pu Y, Werne J P, Meyers P A, Zhang H (2020). Organic matter geochemical signatures of sediments of Lake Ngoring (Qinghai-Tibetan Plateau): a record of environmental and climatic changes in the source area of the Yellow River for the last 1500 years. *Palaeogeogr Palaeoclimatol Palaeoecol*, 551: 109729
- Pu Y, Zhang H, Lei G, Chang F, Yang M, Huang X (2009). *n*-alkane distribution coupled with organic carbon isotope composition in the shell bar section, Qarhan paleolake, Qaidam Basin, NE Tibetan Plateau. *Front Earth Sci China*, 3(3): 327–335
- Pu Y, Zhang H, Lei G, Chang F, Yang M, Zhang W, Lei Y, Yang L, Pang Y (2010). Climate variability recorded by *n*-alkanes of paleolake sediment in Qaidam Basin on the northeast Tibetan Plateau in late MIS3. *Sci China Earth Sci*, 53(6): 863–870
- Ropelewski C F, Halpert M S (1986). North American precipitation and temperature patterns associated with the El Niño/Southern Oscillation (ENSO). *Mon Weather Rev*, 114(12): 2352–2362
- Sheppard P R, Tarasov P E, Graumlich L J, Heussner K U, Wagner M, Österle H, Thompson L G (2004). Annual precipitation since 515 BC reconstructed from living and fossil juniper growth of northeastern Qinghai Province, China. *Clim Dyn*, 23(7): 869–881
- Song C, Huang B, Ke L, Richards K S (2014). Seasonal and abrupt changes in the water level of closed lakes on the Tibetan Plateau and implications for climate impacts. *J Hydrol (Amst)*, 514: 131–144
- Stager J C, Ruzmaikin A, Conway D, Verburg P, Mason P J (2007). Sunspots, El Niño, and the levels of Lake Victoria, East Africa. *J Geophys Res*, 112(D15): D15106
- Tan L, Cai Y, Yi L, An Z, Ai L (2008). Precipitation variations of Longxi, northeast margin of Tibetan Plateau since AD 960 and their relationship with solar activity. *Clim Past*, 4(1): 19–28
- Tian F, Wang Y, Dong J, Yuan L, Tang W (2022). An 1800-year record of lake level and climate change from alkaline lakes in southern Inner Mongolia, China. *J Paleolimnol*, 67(1): 59–73
- Tian H, Lan Y, Wen J, Jin H, Wang C, Wang X, Kang Y (2015). Evidence for a recent warming and wetting in the source area of the Yellow River (SAYR) and its hydrological impacts. *J Geogr Sci*, 25(6): 643–668
- Tian M, Zhao J, Wang J, Li T (2021). Runoff simulation of snowmelt in the Huangheyuan-Dari district of the source region of the Yellow River based on UEB model. *J Qinghai Univ*, 39(02): 98–104 (in Chinese)
- Vieira L E A, Solanki S K, Krivova N A, Usoskin I G (2011). Evolution of the solar irradiance during the Holocene. *Astron Astrophys*, 531: A6
- Walling D E, Fang D (2003). Recent trends in the suspended sediment loads of the world's rivers. *Global Planet Change*, 39(1–2): 111–126
- Wan S, Hu Y, You Z, Kang J, Zhu J (2013). Extreme monthly precipitation pattern in China and its dependence on Southern Oscillation. *Intern J Climat*, 33(4): 806–814
- Wang H, He Y, Liu W, Zhou A, Kolpakova M, Krivonogov S, Liu Z (2019). Lake water depth controlling archaeal tetraether distributions in Midlatitude Asia: implications for paleo lake-level reconstruction. *Geophys Res Lett*, 46(10): 5274–5283
- Wu J, Yu Z, Zeng H, Wang N (2009). Possible solar forcing of 400-year wet-dry climate cycles in northwestern China. *Clim Change*, 96(4): 473–482
- Xu H (2006). Modification of normalised difference water index (NDWI) to enhance open water features in remotely sensed imagery. *Int J Remote Sens*, 27(14): 3025–3033
- Xu J (2018). A cave  $\delta^{18}\text{O}$  based 1800-year reconstruction of sediment load and streamflow: the Yellow River source area. *Catena*, 161: 137–147
- Zhang G, Chen W, Xie H (2019a). Tibetan Plateau's lake level and volume changes from NASA's ICESat/ICESat-2 and Landsat missions. *Geophys Res Lett*, 46(22): 13107–13118
- Zhang G, Luo W, Chen W, Zheng G (2019b). A robust but variable lake expansion on the Tibetan Plateau. *Sci Bull (Beijing)*, 64(18):

- 1306–1309
- Zhang G, Yao T, Shum C K, Yi S, Yang K, Xie H, Feng W, Bolch T, Wang L, Behrangi A, Zhang H, Wang W, Xiang Y, Yu J (2017). Lake volume and groundwater storage variations in Tibetan Plateau's endorheic basin. *Geophys Res Lett*, 44(11): 5550–5560
- Zhang G, Yao T, Xie H, Yang K, Zhu L, Shum C K, Bolch T, Yi S, Allen S, Jiang L, Chen W, Ke C (2020). Response of Tibetan Plateau lakes to climate change: trends, patterns, and mechanisms. *Earth Sci Rev*, 208: 103269
- Zhang P, Cheng H, Edwards R L, Chen F, Wang Y, Yang X, Liu J, Tan M, Wang X, Liu J, An C, Dai Z, Zhou J, Zhang D, Jia J, Jin L, Johnson K R (2008). A test of climate, sun, and culture relationships from an 1810-year Chinese cave record. *Science*, 322(5903): 940–942
- Zhao N, Yan H, Yang Y, Liu C, Ma X, Wang G, Zhou P, Wen H, Qu X, Dodson J (2021). A 23.7-year long daily growth rate record of a modern giant clam shell from South China Sea and its potential in high-resolution paleoclimate reconstruction. *Palaeogeogr Palaeoclimatol Palaeoecol*, 583: 110682
- Zheng H, Zhang L, Zhu R, Liu C, Sato Y, Fukushima Y (2009). Responses of streamflow to climate and land surface change in the headwaters of the Yellow River Basin. *Water Resour Res*, 45(7): W00A19
- Zheng J, Wen Y (2020). Dataset of dry-wet index in the middle and upper reaches of the Yellow River over the past 2000 years. *Digital J Global Change Data Repository*, 2020